A METHOD FOR ESTIMATING LATERAL DIFFUSION COEFFICIENTS IN MEMBRANES FROM STEADY-STATE FLUORESCENCE QUENCHING STUDIES

MARY F. BLACKWELL, KLEONIKI GOUNARIS, STEPHEN J. ZARA, AND JAMES BARBER
Agricultural and Food Research Council Photosynthesis Research Group, Imperial College of Science and Technology, Department of Pure and Applied Biology, London SW7 2BB, England

ABSTRACT The Stern–Volmer theory, in which the quantum yield ratio (I^0/I) depends linearly on the quencher concentration, will typically be inapplicable to fluorescence quenching in membranes. Numerical analysis shows that diffusion-controlled quenching results in a nonlinear concentration dependence for diffusion coefficients less than or of the order of 10^{-6} cm^2s^{-1} and probe fluorescence lifetimes in the region of 10–100 ns. Lateral diffusion coefficients in membranes are typically overestimated an order of magnitude or more by the Stern–Volmer theory. An alternative empirical method is presented, which represents nonlinear concentration curves by a single parameter linear approximation determined by a least-squares analysis. The fitting parameter, P, depends on the interaction distance, the membrane thickness, the maximum extent of quenching and, in the case of biexponential probe fluorescence decay, the fluorescence kinetic parameters. P is presented in tabular form for a useful range of these parameters. The method is used to estimate diffusion coefficients for plastoquinone and plastoquinol from pyrene fluorescence quenching in soya bean phosphatidylcholine liposomes. It is found that the diffusion coefficients are nearly equal and in the region of 1.3–3.5 $\times$ 10^{-7} cm^2s^{-1} for interaction radii of 1.5–0.5 nm, respectively.

INTRODUCTION

Three membrane-bound protein complexes function in linear electron flow in plant photosynthesis: the reaction centers of photosystems (PS) I and II and the cytochrome b_6f complex (1–3). It is believed that PS I and PS II are segregated, with PS II located predominantly in appressed granal regions of the chloroplast thylakoid membrane and PS I restricted to stromal and granal-end lamellae (1–3). This raises the possibility that some redox components, such as plastoquinone and plastoquinol, function as mobile carriers and therefore that the rate of linear electron flow can be determined in part by long-range diffusion. Several publications have addressed this question and proposed plastoquinone diffusion coefficients ranging from 10^{-8} to 10^{-6} cm^2s^{-1} (2, 4–6), but there have been no reports of actual measurements. This is due in part to the inadequacy of current methods when applied to small diffusants in liposomes or subcellular organelles, evident in the striking disagreement among results for related molecules, e.g., $\sim 10^{-9}$ cm^2s^{-1} for a fluorescent derivative of benzoquinone (7), and 10^{-6}–10^{-5} cm^2s^{-1} for ubiquinones (8, 9).

One method for measuring diffusion coefficients in such systems that deserves further development is probe fluorescence quenching. Fluorescence quenching is readily observed in membranes, e.g., pyrene excimer formation (10–12) and anthracene fluorescence quenching by quinones (8, 9, 13), and the experimental methods are simple and straightforward. However, the theory of dynamic fluorescence quenching in membranes is not fully developed, and the theory for isotropic solution has been used without modification for data analysis (8, 9, 13). It is typically the case in isotropic solution that diffusion-controlled ("dynamic") quenching can be described by the Stern–Volmer theory, in which the reciprocal of the fluorescence quantum yield depends linearly on the quencher concentration (14, 15). The slope ("Stern–Volmer constant") is related to diffusion coefficients by the Smoluchowski equation (15). Nonlinearity results from either "static" or "transient dynamic" quenching, or a combination of the two, and is not easy to interpret (15). Numerical analysis has shown that the theory of dynamic quenching in membranes, while of approximately the same form, differs from the isotropic theory, and a Stern–Volmer-type treatment has been defined (16). However, this approach may not be as useful in membranes, in that significant nonlinearity, attributed to static quenching, has been reported (8, 9, 13).

In this paper, we report the observation of pyrene fluorescence quenching by plastoquinone and plastoquinol in phosphatidylcholine (PC) liposomes. To obtain estimates of diffusion coefficients, it was necessary to develop

Please address all correspondence to Dr. Blackwell, whose present address is Department of Plant Biology, U. S. Department of Agriculture/ Agricultural Research Service, University of Illinois, Urbana, IL 61801.

further the theory of fluorescence quenching in membranes, and we report the results of a numerical analysis of the concentration dependence of the fluorescence quantum yield resulting from dynamic quenching. The analysis shows that nonlinear dynamic quenching is typical rather than exceptional in membrane systems and that the Stern–Volmer-type quenching constant is a poor approximation, resulting in overestimation of diffusion coefficients by up to orders of magnitude. We describe an empirical method for estimating diffusion coefficients from quenching data.

THEORETICAL SECTION

Theory of Dynamic Fluorescence Quenching in Fluid Sheets

The simplest appropriate model describes the membrane space as a continuous fluid sheet with local cylindrical symmetry (16). The quantity of interest in steady-state quenching experiments is the ratio (16)

$$Q = \frac{I^0}{I} = \frac{\int_0^\infty \exp(-t/t_0)\,dt}{\int_0^\infty \exp\left\{-\left[t/t_0 + \int_0^t J_Q(s)\,ds\right]\right\} dt}, \quad (1)$$

which defines Q, with I^0 and I the respective intensities of fluorescence in the absence and presence of quenching, t_0 the fluorescence lifetime in the absence of quenching, and

$$\int_0^t J_Q(s)\,ds = gcF(t/t_Q)$$

with

$$F(t/t_Q) = \int_0^\infty \frac{(1 - \exp(-x^2 t/t_Q))}{J_0^2(x) + Y_0^2(x)} \frac{dx}{x^3}.$$

In Eq. 1, $g = 8N_0hR^2/\pi$ in which N_0 is Avogadro's number in units of $mmol^{-1}$, h the membrane thickness, and R the interaction distance; c is the average quencher concentration in units of mmol cm^{-3}; $t_Q = R^2/D$ with D the coefficient of relative diffusion parallel to the membrane surface, $D = D_p + D_Q$ (17), and D_p and D_Q the lateral diffusion coefficients of probe and quencher, respectively; and J_0 and Y_0 are Bessel functions of the first and second kind, respectively. Eq. 1 assumes Smoluchowski boundary conditions (14, 16, 18), which are valid for diffusion-controlled reactions (17).

It is not possible to perform the integration in the denominator of Eq. 1. Thus Owen (16) found an integrable approximation to $F(t/t_Q)$ of the form

$$F(t/t_Q) \simeq f_1 t/t_Q + f_2 (t/t_Q)^{1/2}, \quad (2)$$

where f_1 and f_2 are numerically determined fitting factors, and the result is analogous to the isotropic one (14, 16)

$$Q \simeq Q' = \frac{a}{1 - \beta}, \quad (3)$$

which defines Q', where

$$a = 1 + \frac{8N_0hDct_0f_1}{\pi}$$

$$\beta = b(\pi a)^{-1/2} \exp(b^2/a)\, erfc\,(ba^{-1/2})$$

$$2b = ct_0Rf_2D^{1/2}$$

$$erfc(x) = 2\pi^{-1/2}\int_x^\infty \exp(-t^2)\,dt.$$

Both Q and Q' generally show a nonlinear dependence on the quencher concentration. The linear, Stern–Volmer-type case occurs when $\beta \ll 1$, and

$$Q' \simeq Q'' = a, \quad (4)$$

which defines Q''. The slope of Eq. 4,

$$m'' = \frac{dQ''}{dc} = \frac{8N_0hDt_0f_1}{\pi}, \quad (5)$$

is the two-dimensional analogue of the Stern–Volmer quenching constant.

The nonlinear case, $\beta \sim 1$, corresponds to significant transient dynamic quenching (15). This needs to be distinguished from static quenching (13, 15), which causes a similar nonlinear concentration dependence and has not been included here. Conclusive evidence for quenching being entirely dynamic is that the decrease in steady-state intensity corresponds quantitatively to an increased rate of fluorescence emission (15). Such studies are not possible at present because the theory of quenching kinetics in membranes has not been elucidated. The isotropic method (13) for determining the contribution from static quenching is inapplicable, because the kinetic contribution from transient dynamic quenching is obviously not negligible when dynamic quenching concentration curves are nonlinear, which is shown in the next section to be typical in membrane systems.

Numerical Results

Calculations were carried out on a Cray 1S computer using the COS 1.14 operating system. Error functions, $erfc(x)$, were calculated using the program AGAUSS listed by Bevington (19). Bessel functions were computed using the programs BESY and BESJ in the IBM Scientific Subroutines Package (20). Integrals were computed by Simpson's rule using the program QSF in the IBM Scientific Subroutines Package (20). Least-squares analysis was carried out using the program CURFIT listed by Bevington (19), which uses the Marquardt algorithm.

The integral in $F(t/t_Q)$ is divergent (18), and its numerical value depends on both the integration limit and the number of intervals chosen for the computation. The fitting factors f_1 and f_2, determined by nonlinear least squares analysis of $F(t/t_Q)$, are slowly convergent and have

the values

$$f_1 = 0.653,\ f_2 = 2.85, \tag{6}$$

at a limit of $x = 20$ with 10^5 intervals, used in subsequent calculations. These are reasonably close to the values $f_1 = 0.622$, $f_2 = 2.78$ obtained by Owen under unspecified conditions (16). Integrals in the quantum yield ratios Q and Q' were rapidly convergent, and calculations were routinely carried out using 300 intervals and a limit of $t = 6t_0$.

Table I shows the quencher concentrations calculated for $Q = 1.25$–5, i.e., 20–80% quenching, and probe fluorescence lifetimes of 1, 10, or 100 ns, assuming an interaction radius of 1 nm. The concentrations are proportional to the diffusion coefficient and inversely proportional to the probe fluorescence lifetime. It is clear from these data that steady-state quenching will often be observable in membranes, where the diffusion coefficients are likely to be of the order 10^{-6} cm^2s^{-1} or less, but that fluorescence lifetimes of 100 ns or longer may be required to observe fluorescence quenching at reasonably low concentrations.

Fig. 1 *A* shows the concentration dependence of Q and Q' (curves *a*) as well as Q'' (curves *b*) for up to 50% quenching. Q' becomes a poorer approximation to Q as the diffusion coefficient is lowered, reflecting inadequacies in the assumptions leading to Eq. 2. However, a more serious difficulty is the divergence of Q and Q' from the Stern–Volmer-type concentration dependence of Q'' in curves *b*. This divergence reflects the magnitude of transient dynamic quenching, as indicated by the concentration dependence of the factor $1/(1 - \beta)$ shown in Fig. 1 *B*. For a fluorescence lifetime of 100 ns, curves *b* from top to bottom correspond to diffusion coefficients of 10^{-6}, 10^{-7}, and 10^{-8} cm^2s^{-1}, respectively, assuming $R = 1$ nm and $h = 5$ nm. For shorter fluorescence lifetimes, the respective values of D would be higher. It is concluded that transient dynamic quenching will make a sizeable, even dominant, contribution to dynamic quenching in membranes, and concentrations curves will typically be nonlinear.

Although Q is not a linear function of concentration, the regression coefficient is 0.98 or better for $Q < 5$ and the curvature will not always be apparent experimentally, given a likely overall error of ±10% in measurements of

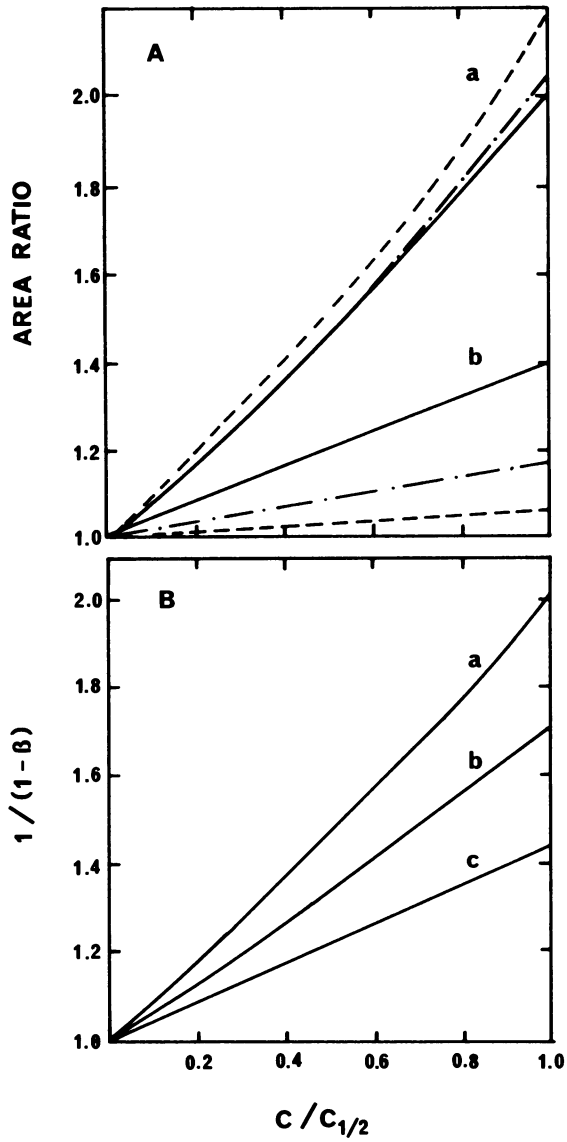

FIGURE 1 Theoretical dependence of fluorescence quenching parameters on the quencher concentration for up to 50% quenching ($Q_{MAX} = 2$). (*A*) Concentration dependence of the area ratios Q, Q', and Q'' in Eqs. 1–4 of the text. (*a*) Q' at $t_0/t_Q = 0.1$ (------), 1.0 (—·—·), and 10 (——), and Q at all values of t_0/t_Q (——). (*b*) Q'' at $t_0/t_Q = 0.1$ (------), 1.0 (—·—·), and 10 (——). (*B*) The deviation from a Stern–Volmer-type concentration dependence. The factor $1/(1 - \beta)$ at $t_0/t_Q = 0.1$ (*a*), 1.0 (*b*), and 10 (*c*). $c_{1/2}$ is the concentration at which $Q = 2$. Other symbols are defined in text.

TABLE I
TYPICAL VALUES OF CONCENTRATIONS AND DIFFUSION COEFFICIENTS IN THE REGION t_0/t_Q = 0.1–10, ASSUMING AN INTERACTION DISTANCE OF 1 NM AND A MEMBRANE THICKNESS OF 5 NM

Concentration (mmol l^{-1})			Diffusion coefficient (cm^2s^{-1})		
$Q = 1.25$	$Q = 2$	$Q = 5$	$t_0 = 100$ ns	$t_0 = 10$ ns	$t_0 = 1$ ns
2	8	21	10^{-6}	10^{-5}	10^{-4}
9	33	87	10^{-7}	10^{-6}	10^{-5}
32	130	340	10^{-8}	10^{-7}	10^{-6}

fluorescence quenching. We therefore found an empirical linear relationship of the form

$$Q \simeq Q_L = Q'' + Pc(m'')^{1/2}, \tag{7}$$

with Q'' and m'' calculated as in the previous section and P a fitting parameter determined by nonlinear least squares analysis. Fig. 2 *a* compares concentration curves for Q and the linear approximation Q_L calculated for $0 < Q < 2$ and indicates that the difference between Q and Q_L will usually be within the expected error. The concentration depen-

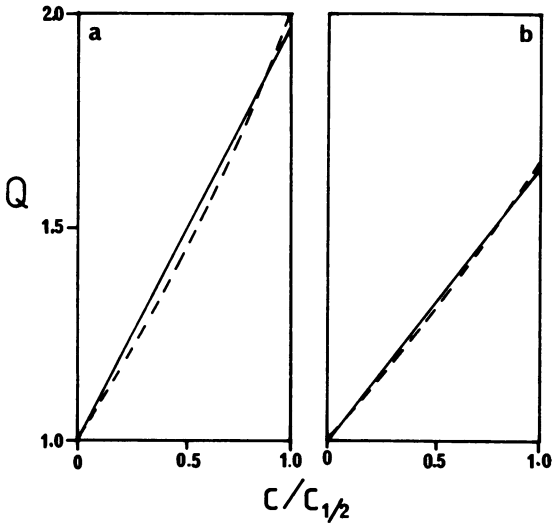

FIGURE 2 Theoretical dependence of the steady-state fluorescence intensity ratio Q on the concentration of quencher for up to 50% quenching (Q_{MAX} = 2). The numerical value of Q in Eq. 1 (*solid curves*) and the linear approximation Q_L in Eq. 7 (*dashed curves*) assuming: (*a*) single exponential fluorescence decay, and (*b*) two exponential decay, with 17% decaying at the same rate as in *a* and 83% decaying 10 times as fast. $c_{1/2}$ is the concentration at which Q = 2 (*a*) or Q_1 = 2 (*b*), with Q_1 as defined for Eq. A1.

dence of Eq. 7 is

$$m = \frac{dQ_L}{dc} = m'' + P(m'')^{1/2}. \quad (8)$$

The slope m is set equal to that determined by linear regression analysis of experimental concentration curves and used in the formula

$$m'' = \tfrac{1}{4}[(P^2 + 4m)^{1/2} - P]^2 \quad (9)$$

to obtain the Stern–Volmer parameter m''. In solving Eq. 8 the positive root was chosen so that $m = m''$ when $P = 0$. Diffusion coefficients can then be estimated using Eq. 5. As described in the Appendix, biexponentially decaying probes are treated as follows. Biexponential fitting parameters, denoted $P^{(2)}$, are obtained from P by correction factors and t_0 in Eq. 5 is replaced by t_1, the lifetime of the slower component. Fig. 2 *b* compares Q and Q_L calculated for biexponential decay in which the slow component lifetime is the same as in Fig. 2 *a* and the fast component decays 10 times as fast with an amplitude of 83%. The agreement between Q and Q_L indicates that diffusion coefficients can be estimated to a high degree of accuracy using the parameters of the longer-lived component, even when it makes a minor contribution to the decay kinetics.

The fitting parameter P has several dependences. First, P depends upon Q_{MAX}, the maximum value of Q in a particular experimental plot. Second, P depends on the ratio t_0/t_Q at or below ~0.5, but this will not be important at physiologically reasonable concentrations. Third, P depends on the value of g in Eq. 1, i.e., the values assumed for the membrane thickness and the interaction radius. This results in an inverse dependence of D on R, as in the isotropic theory.

TABLE II
VALUES OF THE FITTING PARAMETER P IN EQ. 7, DETERMINED NUMERICALLY AS DESCRIBED IN THE TEXT

R	Q_{MAX}					
	1.25	1.5	2.0	3.0	4.0	5.0
nm						
0.5	4.573	4.877	5.413	6.315	7.071	7.716
1.0	9.162	9.772	10.846	12.653	14.166	15.459
1.5	13.742	14.657	16.268	18.977	21.248	23.188

R is interaction distance, and Q_{MAX} is the maximum value of Q in Eq. 1 in a concentration plot.

Table II lists values of P calculated, assuming a membrane thickness of 5 nm and interaction radii of 0.5, 1, and 1.5 nm in the region of $1.25 < Q_{MAX} < 5$, which we found to be most relevant experimentally for pyrene fluorescence quenching in membranes. In general Q_{MAX} has a value intermediate to those listed in Table II, and P is determined by linear interpolation (21). A table of values of P calculated for $1 < g < 40$ and $1.25 < Q_{MAX} < 5$ is presented in the Appendix.

Fig. 3 shows the theoretical dependence of the diffusion coefficient on the experimental slope m. The Stern–Volmer-type estimate corresponds to $P = 0$ and consequently to a linear dependence of D on m (curve *a*). The curves for $P > 0$ fall below the Stern–Volmer curve and show upward curvature (curves *b–d*). Slopes of 120 and 20

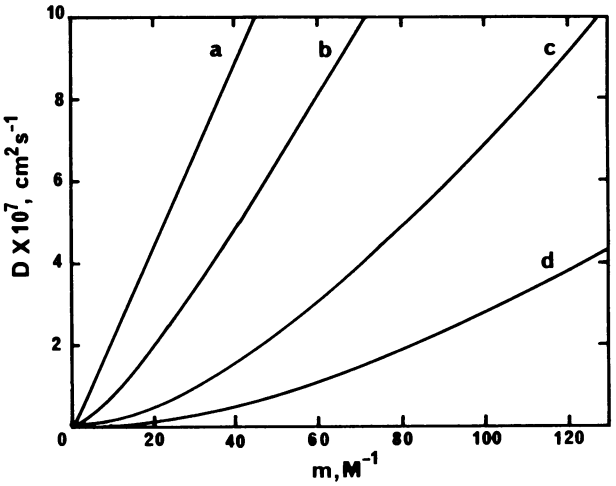

FIGURE 3 Theoretical dependence of diffusion coefficients estimated using Eqs. 5 and 9 and Table AI on the slope m of fluorescence quenching concentration curves. (*a*) When the quantum yield ratio displays a Stern–Volmer-type concentration dependence, $m = m''$ and $P = 0$ in Eq. 9; (*b–d*) when the quantum yield ratio deviates from the Stern–Volmer case, with g = 1 (R ~ 0.4 nm, P = 3.9) (*b*), g = 10 (R ~ 1 nm, P = 12.4) (*c*), and g = 40 (R ~ 2 nm, P = 24.7) (*d*), assuming a membrane thickness of 5 nm and a fluorescence lifetime of 100 ns.

M^{-1} correspond to 50% quenching at 8 and 50 mM quencher concentration, respectively, so that the abscissa in Fig. 3 covers a reasonable experimental range. We conclude that the Stern–Volmer theory will typically overestimate diffusion coefficients in membranes and can do so by up to orders of magnitude.

EXPERIMENTAL SECTION

Materials and Methods

Plastoquinone-9 was a generous gift from Hoffmann-La Roche Inc. (Basel, Switzerland). Plastoquinol-9 was prepared from plastoquinone-9 by the method of Rich (22). Pyrene and soya bean PC (~99%) were used as purchased from Sigma Chemical Co., (Poole, England). Lipid concentrations were routinely determined by gas-liquid chromatography as described previously (23). Concentrations of plastoquinone and plastoquinol were determined by spectrophotometric assay using Crane's extinction coefficients (24).

Model membranes were prepared as follows. Appropriate amounts of PC, pyrene, and plastoquinone or plastoquinol were combined from stock solutions in organic solvents. After complete evaporation of the solvent under a stream of nitrogen, the mixtures were dispersed into distilled water (pH 5) by ultrasonication. Under these preparation conditions, aqueous PC dispersions should consist of liposomes in a broad distribution of sizes (25). The extent of incorporation of plastoquinone and plastoquinol was determined by the fluorescence quenching method described by Fato et al. (9). Partition coefficients greater than 10^4 were obtained. Extent of pyrene incorporation was determined previously (26). The concentrations of plastoquinone, plastoquinol, and pyrene in the membrane were estimated as nanomoles per microgram lipid, assuming a lipid density of 1 g cm^{-3} as described previously (26). Plastoquinol stability to oxidation in PC liposomes was checked by fluorescence assay (27).

Fluorescence measurements were made at room temperature (23°–24°C). Pyrene fluorescence emission was measured at 390 nm as described previously (26).

RESULTS AND DISCUSSION

Fig. 4 shows steady-state fluorescence intensity ratios for pyrene fluorescence quenching in PC liposomes plotted as a function of the concentration of plastoquinone (curve *a*) or plastoquinol (curve *b*) in six experiments. In the region of $1 < Q < 1.5$, the curves are reasonably linear, indicated by the solid lines that represent the average slope below 0.01 M quencher concentration. The curves begin to show saturation above 0.01 M, i.e., when the PC/quencher molar ratio is less than ~125. This is in contrast to the theoretical prediction, as well as reports (8, 9, 13), of upward curvature for quenching in membranes and may reflect failure of the theoretical model or more complex phenomena such as phase partition or micelle formation. The quencher concentration can be arbitrarily high in theory but is limited in reality, and how such effects may be included in the theoretical description is not clear at present. However, it seems reasonable to equate the slope in the linear region to m in Eq. 8 and to use the method outlined above to estimate diffusion coefficients.

The kinetics of pyrene emission at 390 nm in the absence of quencher were determined by least-squares analysis assuming biexponential decay, as reported previously (26). The amplitudes of the two phases of pyrene fluorescence decay are somewhat variable (26). Pyrene fluorescence decay parameters in the absence of quencher were determined in six control samples for each of the experiments shown in Fig. 4, and average values are presented in Table III. Fig. 5 shows that the pyrene fluorescence emission rate in the presence of plastoquinone (curve *b*) or plastoquinol (curve *c*) is obviously increased relative to the rate observed

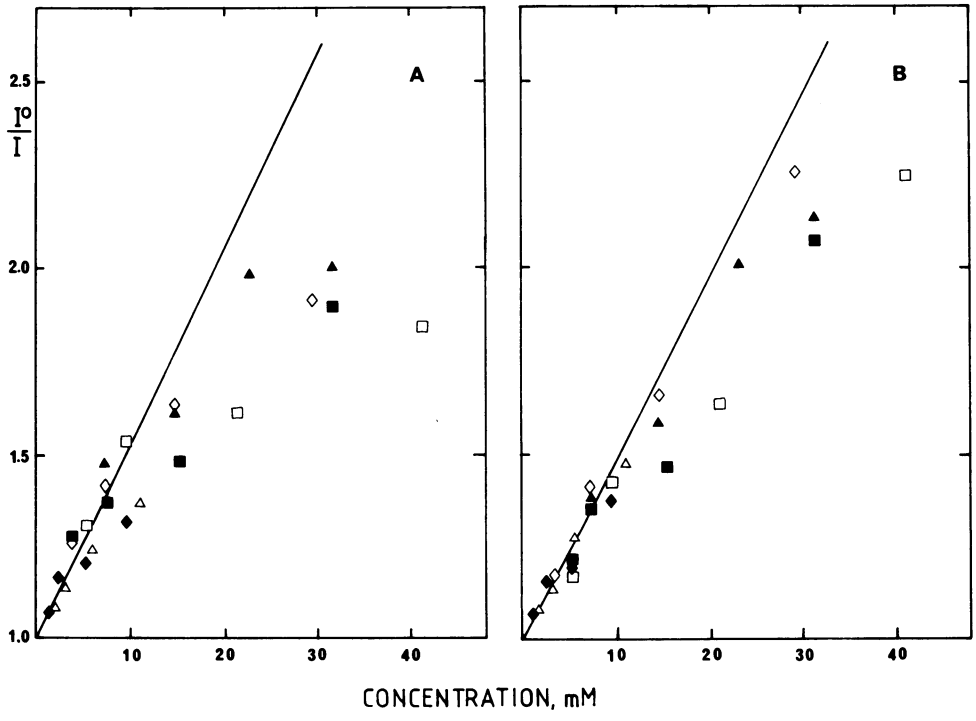

FIGURE 4 Experimental plots of the pyrene steady-state fluorescence intensity ratio as a function of the concentration of plastoquinone (*A*) or plastoquinol (*B*) in soya bean phosphatidylcholine liposomes at lipid concentrations of 100 (◇), 150 (□), 200 (■,▲), 250 (△), and 300 (♦) μg cm^{-3}. The pyrene concentration in the suspensions was 0.5 μM.

TABLE III
ESTIMATION OF DIFFUSION COEFFICIENTS FOR THE SIX EXPERIMENTS IN FIG. 4

Exp. no.	A_1	t_2	t_1	Plastoquinone				Plastoquinol			
				Q_{MAX}	m	$P^{(2)}$	$D \times 10^7$	Q_{MAX}	m	$P^{(2)}$	$D \times 10^7$
		ns	ns		M^{-1}		cm^2s^{-1}		M^{-1}		cm^2s^{-1}
I	0.575	71.81	154.3	1.42	58.34	8.01	2.76	1.42	58.36	8.01	2.76
II	0.703	62.82	148.5	1.32	31.17	8.34	1.05	1.39	38.24	8.48	1.43
III	0.578	72.51	147.2	1.54	55.59	8.27	2.62	1.43	45.30	8.08	1.97
IV	0.495	70.98	149.3	1.39	53.09	7.64	2.60	1.36	49.21	7.59	2.34
V	0.753	54.56	153.6	1.24	41.08	8.40	1.56	1.28	47.89	8.45	1.96
VI	0.611	73.94	159.4	1.49	50.10	8.29	2.06	1.39	54.60	8.11	2.40

The kinetic parameters from two exponential fits of the form $A_1 \exp(-t/t_1) + (1 - A_1) \exp(-t/t_2)$ are presented as averages of six determinations. Q_{MAX} is the maximum value of Q in a concentration plot; m is experimental slope determined by linear regression on data points in Fig. 4 below 0.01 M quencher concentration; $P^{(2)}$ is biexponential fitting parameter determined by the method described in the Appendix; D is the diffusion coefficient estimated by the method described in the text, assuming an interaction radius of 1 nm.

in the absence of quencher (curve *a*). The emission rate is proportional to the quencher concentration (data not shown). This is evidence that the quenching is not a trivial or "inner filter" effect and does not reflect Förster-type energy transfer (28). It is also evidence that quenching is partially or entirely dynamic. As discussed in the Theoretical Section, the kinetic theory of quenching in membranes has not been elucidated. Therefore we did not undertake a detailed study of the concentration dependence of the fluorescence kinetics for the present study. We assume that only dynamic and transient dynamic quenching contribute to Fig. 4.

Table III presents the data used in the six estimations of D for plastoquinone and plastoquinol in PC liposomes. The values of $P^{(2)}$ were calculated from the values of P in Table II using the method described in the Appendix, assuming a membrane thickness of 5 nm and an interaction radius of 1 nm. Diffusion coefficients were then estimated using the method described in the Theoretical Section. The average values of the diffusion coefficients in Table III are 2.11 ± 0.31 and 2.14 ± 0.21 × 10^{-7} cm^2s^{-1} for plastoquinone and plastoquinol, respectively. The estimates of D are in the region 3.5–1.3 × 10^{-7} cm^2s^{-1} when R is in the region 0.5–1.5 nm, showing an R^{-1} dependence as in the isotropic theory. Previous estimates in PC liposomes (29) were erroneous.

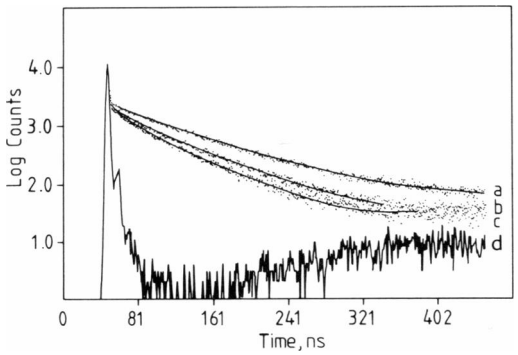

FIGURE 5 Kinetics of pyrene fluorescence emission at 390 nm in the absence of quencher (*a*) and in the presence of plastoquinol (*b*) or plastoquinone (*c*) at respective concentrations of 24 and 26 mM in soya bean phosphatidylcholine liposomes. The lamp profile is shown in *d*. The pyrene and lipid concentrations in the suspension were 0.5 μM and 200 μg cm^{-3}, respectively.

The calculation of values in Table III assumes that the diffusion coefficient of pyrene may be neglected compared with those of plastoquinone and plastoquinol, so that $D = D_Q$. We previously determined that the upper limit for the pyrene excimer formation rate constant, k_e, is 10^6 $M^{-1}s^{-1}$ (26). The rate constants, k_Q, of pyrene fluorescence quenching reported here are of the order 10^8 $M^{-1}s^{-1}$. Regardless of the form of the Smoluchowski equation in membranes, which has not been satisfactorily determined, there is little doubt that $k_e \ll k_Q$ implies $D_p \ll D_Q$.

CONCLUSION

By numerical analysis, we have determined the dependence of the fluorescence quantum yield on the quencher concentration for diffusion-controlled quenching in membranes. Concentration curves are typically nonlinear owing to a significant contribution from transient dynamic quenching. The Stern–Volmer quenching constant, m'' in Eq. 5, is a poor approximation to the slope, m, of quenching concentration curves and the assumption that $m = m''$ results in significant overestimation of lateral diffusion coefficients less than ~10^{-6} cm^2s^{-1} for probe fluorescence lifetime of 10 ns or greater. Thus the isotropic theory, which has been used to describe quenching in membranes (8, 9, 13), will typically result in significant overestimation of diffusion coefficients.

The empirical method presented in this paper results in an estimate of 2.6 × 10^{-7} cm^2s^{-1} for the diffusion coefficient of ubiquinone-10 in asolectin liposomes, using the data of Fato et al. (9), i.e., $m = 22$ M^{-1}, $t_0 = 9.4$ ns, $Q_{MAX} \sim 3$, and $D_p = 2.5 \times 10^{-7}$ cm^2s^{-1}, assuming $R = 1$ nm and $h = 5$ nm, with $m = k_m t_0$. This value is more than an order of magnitude smaller than estimates based on the isotropic theory (9), but in good agreement with values presented

here for plastoquinone and plastoquinol in PC liposomes. This invariance of D and therefore of the reaction rate is evidence that fluorescence quenching is diffusion controlled. If the reaction rate is determined entirely by diffusion, the reaction rate constant is essentially invariant for quenchers of widely varying chemical structure (28). A dependence of the reaction rate on the nature of the quencher, on the other hand, implies a significant activational barrier and chemical or mixed control of the reaction rate. We cannot explain the observation that ubiquinol does not quench anthroylstearate fluorescence (13).

Steady-state fluorescence measurements are simple and far less time-consuming than kinetics measurements for routine measurements of quenching. However, experimental and theoretical studies of the kinetics of quenching in membranes are required to establish the validity of the steady-state method, especially concerning the extent of the contribution from static quenching. Preliminary work indicates that both experimental and theoretical fluorescence decays in the presence of quenching can be fit reasonably by a biexponential decay function, but the fitting parameters do not have a simple relationship to the rate of quenching. Thus, fluorescence kinetics studies require modification of software for analysis of experimental curves. Such studies are necessary but beyond the scope of the present paper.

The diffusion coefficients determined by fluorescence quenching are about two orders of magnitude higher than the value obtained by microphotolysis using a fluorescent derivative of ubiquinone (17). It is clear from the data in Table I that a diffusion coefficient of the order 10^{-8} cm^2s^{-1} or less would not result in detectable dynamic quenching at the concentrations used in the present or previous (8, 9, 13) studies, and the observed decreases in steady-state fluorescence intensity would have to be attributed entirely to static quenching. While the contribution from static quenching cannot be determined quantitatively at present, the observations reported here and elsewhere (13) of increases in fluorescence emission rates in the presence of quenchers are consistent with a sizeable contribution from dynamic quenching and therefore incompatible with lateral diffusion coefficients of the order 10^{-9} cm^2s^{-1}. It is possible that the fluorescence tag used in the microphotolysis studies retards the motion of ubiquinone, most likely by increasing the activational barrier to diffusion, which can be determined by studying its temperature dependence.

From the diffusion coefficients measured here it is possible to estimate a theoretical diffusion pathlength by the 2D Einstein–Smoluchowski equation (28), $r = 2(Dt)^{1/2}$, where r is the root-mean-square displacement in time t. According to the flash absorption studies of Haehnel (2), the halftime for diffusion between the binding sites on PS II and cytochrome b_6f has an upper limit of 2–3 ms corresponding to a theoretical pathlength of ~360–590 nm using the values estimated here for D. The true pathlength may be as small as 20 nm (30) or as great as 500–1,000 nm (2, 3), depending on the contribution of plastoquinol to long-range electron transport as well as its distribution relative to cytochrome b_6f complexes that are functional in linear electron flow. The diffusion coefficients reported

TABLE AI
VALUES COMPUTED FOR THE FITTING PARAMETER P IN EQ. 7 OF THE TEXT AT VARIOUS VALUES OF g IN EQ. 1 AND Q_{MAX}

g	P					
	Q_{MAX} = 1.25	Q_{MAX} = 1.5	Q_{MAX} = 2	Q_{MAX} = 3	Q_{MAX} = 4	Q_{MAX} = 5
1	3.31	3.53	3.92	4.57	5.12	5.58
2	4.68	4.94	5.55	6.46	7.24	7.90
3	5.73	6.04	6.78	7.91	8.86	9.67
4	6.62	7.06	7.83	9.14	10.2	11.2
5	7.40	7.86	8.73	10.2	11.4	12.5
6	8.10	8.67	9.59	11.2	12.5	13.6
7	8.75	9.27	10.4	12.1	13.5	14.8
8	9.36	9.98	11.1	12.9	14.5	15.8
9	9.93	10.6	11.7	13.7	15.3	16.7
10	10.5	11.2	12.4	14.5	16.2	17.7
12	11.5	12.2	13.6	15.8	17.7	19.3
14	12.4	13.2	14.7	17.1	19.1	20.9
16	13.2	14.1	15.7	18.3	20.5	22.3
18	14.0	14.9	16.7	19.3	21.7	23.7
20	14.8	15.7	17.6	20.4	22.9	25.0
25	16.5	17.6	19.6	22.8	25.6	27.9
30	18.1	19.3	21.4	25.1	28.0	30.6
35	19.6	20.9	23.1	27.2	30.3	33.0
40	20.9	22.3	24.7	29.2	32.3	35.3

Symbols are defined in the text.

TABLE AII

THE SLOPES, df/dQ_{MAX}, AND INTERCEPTS DETERMINED FROM NUMERICAL ANALYSIS OF $f = P^2/P$

y_2^0/y_1^0	t_2/t_1				
	0.1	0.2	0.3	0.4	0.5
0.1	−0.029970, 0.91948	−0.019874, 0.92710	−0.013412, 0.93537	−0.008929, 0.94421	−0.0057483, 0.95332
0.2	−0.045711, 0.84304	−0.030923, 0.86092	−0.021190, 0.87845	−0.014291, 0.89594	−0.0092940, 0.91343
0.3	−0.053805, 0.77351	−0.36997, 0.80210	−0.025678, 0.82852	−0.017511, 0.85404	−0.011505, 0.87907
0.4	−0.057567, 0.71118	−0.040137, 0.74997	−0.028167, 0.78464	−0.019395, 0.81746	−0.012860, 0.84922
0.5	−0.058789, 0.65554	−0.04141, 0.70374	−0.029403, 0.74592	−0.020424, 0.78532	−0.013655, 0.82309
0.6	−0.058490, 0.60586	−0.041736, 0.66261	−0.029840, 0.71159	−0.020893, 0.75690	−0.014077, 0.80004
0.7	−0.057278, 0.56139	−0.041286, 0.62587	−0.029761, 0.68098	−0.020993, 0.73162	−0.014246, 0.77958
0.8	−0.055519, 0.52144	−0.040399, 0.59290	−0.029348, 0.65356	−0.020846, 0.70899	−0.014244, 0.76129
0.9	−0.053447, 0.48540	−0.039244, 0.56319	−0.028718, 0.62887	−0.020535, 0.68864	−0.014123, 0.74485
1.0	−0.051206, 0.45278	−0.037928, 0.53630	−0.027952, 0.60653	−0.020116, 0.67025	−0.013923, 0.73001
1.1	−0.048893, 0.42312	−0.036524, 0.51185	−0.027103, 0.58624	−0.019628, 0.65354	−0.013668, 0.71654
1.2	−0.046567, 0.39606	−0.035081 0.48955	−0.026208 0.56772	−0.019095 0.63831	−0.013377 0.70426
1.3	−0.044268, 0.37128	−0.033629, 0.46912	−0.025291, 0.55077	−0.018539, 0.62436	−0.013064, 0.69302
1.4	−0.04202, 0.34852	−0.032191, 0.45035	−0.024370, 0.53519	−0.017971, 0.61155	−0.012738, 0.68270
1.5	−0.039838, 0.32754	−0.030780, 0.43304	−0.023457, 0.52083	−0.017401, 0.59974	−0.012405, 0.67318
2.0	−0.030109, 0.24335	−0.024349, 0.36353	−0.019206, 0.46312	−0.014683, 0.55229	−0.010774, 0.63498
3.0	−0.015968, 0.13780	−0.014719, 0.27620	−0.012659, 0.39055	−0.010371, 0.49260	−0.008095, 0.58695
4.0	−0.0065826, 0.074479	−0.0081965, 0.22368	−0.0081397, 0.34684	−0.0073362, 0.45663	−0.0061700, 0.55800
5.0	0.00002212, 0.032310	−0.0035694, 0.18864	−0.0049012, 0.31766	−0.0051401, 0.43261	−0.0047617, 0.53865

The entries are listed in the order slope, intercept. $t_2(t_1)$ is fluorescence lifetime of shorter (longer)-lived component of biexponential decay of the form of Eq. AI; y_2^0 (y_1^0) is fluorescence quantum yield of component 2 (1) in the absence of quenching. Further details in the text.

here are consistent with a role in long-range transport but not large enough to eliminate the possibility that plastoquinol diffusion determines the rate of linear electron flow.

APPENDIX

Values of the fitting parameter P in Eq. 7 in the case of monoexponential decay kinetics are presented in Table AI for $1 < g < 40$ and $1.25 < Q_{MAX} < 5$. The values in Tables II and AI are the average of P computed at $t_0/t_Q = 10$ and 1, which were generally within 3–5% of one another, depending on Q_{MAX}. Values of P for intermediate values of g and Q_{MAX} may be determined by linear interpolation (21).

When the fluorescence decay in the absence of quenching is biexponential and of the form

$$I(t) = A_1 \exp(-t/t_1) + A_2 \exp(-t/t_2), \qquad \text{(A1)}$$

Eq. 1 is rewritten in terms of the longer-lived component, henceforth assumed to be component 1, as

$$Q = \frac{Q_1}{y_1^0 + y_2^0 Q_1/Q_2}, \qquad \text{(A2)}$$

with Q_i the quenching ratio of component i separately, i.e.,

$$Q_i = \frac{\int_0^\infty I_i^0(t)\,dt}{\int_0^\infty I_i(t)\,dt},$$

and y_i^0 the quantum yield of fluorescence from component i in the absence of quenching

$$y_i^0 = \frac{A_i t_i}{A_1 t_1 + A_2 t_2}.$$

The Q_i were determined numerically as described in the Theoretical Section and values of $P^{(2)}$, the fitting parameter for biexponential decay kinetics, were determined by linear regression analysis as in Eq. 7. Correction factors, $f = P^{(2)}/P$, were then calculated to allow values of $P^{(2)}$ to be determined conveniently from the values of P presented in Tables II and AI. It was found that f depends on the fluorescence kinetic parameters and the value of Q_{MAX}, but is independent of R and h. Therefore, values of the slopes, df/dQ_{MAX}, and intercepts determined from numerical analysis of f are presented in Table AII. The determination of $P^{(2)}$ requires knowledge of y_2^0/y_1^0, t_2/t_1, and Q_{MAX} and proceeds as follows. Step 1: The value of df/dQ_{MAX} and intercept for a particular set of kinetic parameters is determined from Table AII by linear interpolation (21). Step 2: The slope and intercept from step 1 are used to calculate f at Q_{MAX} values in Table II or AI on either side of the experimental Q_{MAX}. Step 3: The correction factors from step 2 are used to calculate values of $P^{(2)}$ corresponding to the tabulated values of P. Step 4: The value of $P^{(2)}$ at the experimental Q_{MAX} is obtained from the values obtained in step 3 by linear interpolation (21). Numerical analysis shows that this procedure results in an error of 5% or less in estimates of D, compared with the exact numerical value, for experimental slopes of 2.5 M^{-1} or more.

We are grateful to Professor Sir George Porter of the Royal Institution for useful discussions.

M. F. Blackwell was supported by the U. S. Department of Health and Human Services, National Research Service Award F32-GM09815 from the National Institute of General Medical Sciences. We acknowledge support from the Science and Engineering Research Council, the Agricultural and Food Research Council, and the Royal Society.

Received for publication 11 December 1986 and in final form 23 January 1987.

REFERENCES

1. Barber, J. 1985. Thylakoid membrane structure and organization of electron transport components. *In* Photosynthetic Mechanism and the Environment. Vol. 6. Topics in Photosynthesis. J. Barber and N. R. Baker, editors. Elsevier North-Holland Biomedical Press, Amsterdam. 91–134.
2. Haehnel, W. 1984. Photosynthetic electron transport in higher plants. *Ann. Rev. Plant Physiol.* 35:659–93.
3. Whitmarsh, J. 1986. Mobile electron carriers in thylakoids. *In* Photosynthesis III. Vol. 19. Encyclopedia of Plant Physiology. L. A. Staehelin and C. Arntzen, editors. Springer-Verlag GmbH & Co., Heidelberg, Berlin. 508–525.
4. Anderson, J. M. 1981. Consequences of spatial separation of photosystem 1 and 2 in thylakoid membranes of higher plant chloroplasts. *FEBS (Fed. Eur. Biochem. Soc.) Lett.* 124:62–66.
5. Barber, J. 1983. Photosynthetic electron transport in relation to thylakoid membrane composition and organization. *Plant Cell Environ.* 6:311–322.
6. Millner, P. A., and J. Barber. 1984. Plastoquinone as a mobile redox carrier in the photosynthetic membrane. *FEBS (Fed. Eur. Biochem. Soc.) Lett.* 169:1–6.
7. Gupte, S., E. S. Wu, L. Hoechli, M. Hoechli, K. Jacobson, A. E. Sowers, and C. R. Hackenbrock. 1984. Relationship between lateral diffusion, collision frequency, and electron transfer of mitochondrial inner membrane oxidation-reduction components. *Proc. Natl. Acad. Sci. USA.* 81:2606–2610.
8. Fato, R., M. Battino, G. P. Castelli, and G. Lenaz. 1985. Measurement of the lateral diffusion coefficients of ubiquinones in lipid vesicles by fluorescence quenching of 12-(9-anthroyl)stearate. *FEBS (Fed. Eur. Biochem. Soc.) Lett.* 179:238–242.
9. Fato, R., M. Battino, M. Degli Esposti, G. P. Castelli, and G. Lenaz. 1986. Determination of partition and lateral diffusion coefficients of ubiquinones by fluorescence quenching of n-(9-anthroyloxy)stearic acids in phospholipid vesicles and mitochondrial membranes. *Biochemistry.* 25:3378–3390.
10. Vanderkooi, J. M., and J. B. Callis. 1974. Pyrene. A probe of lateral diffusion in the hydrophobic region of membranes. *Biochemistry.* 13:4000–4006.
11. Galla, H., and E. Sackmann. 1974. Lateral diffusion in the hydrophobic region of membranes: use of pyrene excimers as optical probes. *Biochim. Biophys. Acta.* 339:103–115.
12. Georgescauld, D., J. P. Desmasez, R. Lapouyade, A. Babeau, H. Richard, and M. Winnik. 1980. Intramolecular excimer fluorescence: a new probe of phase transitions in synthetic phospholipid membranes. *Photochem. Photobiol.* 31:539–545.
13. Chance, B., M. Erecinska, and G. Radda. 1975. 12-(9-Anthroyl)stearic acid, a fluorescent probe for the ubiquinone region of the mitochondrial membrane. *Eur. J. Biochem.* 54:521–529.
14. Yguerabide, J., M. A. Dillon, and M. Burton. 1964. Kinetics of diffusion-controlled processes in liquids. Theoretical consideration of luminescence system: quenching and excitation transfer in collision. *J. Chem. Phys.* 40:3040–3052.
15. Birks, J. B. 1970. Photophysics of Aromatic Molecules. John Wiley & Sons, Inc., New York. Chap. 9.
16. Owen, C. S. 1975. Two dimensional diffusion theory: cylindrical diffusion model applied to fluorescence quenching. *J. Chem. Phys.* 62:3204–3207.
17. Noyes, R. M. 1961. Effects of diffusion rates on chemical kinetics. *Prog. React. Kinet.* 1:129–160.
18. Razi Naqvi, K. 1974. Diffusion-controlled reactions in two-dimensional fluids: discussion of measurements of lateral diffusion of lipids in biological membranes. *Chem. Phys. Lett.* 28:280–284.
19. Bevington, P. R. 1969. Data Reduction and Error Analysis for the Physical Sciences. McGraw-Hill Book Co., New York. 336 pp.

20. S/360 Scientific Subroutine Package Version 3 Programmer's Manual. IBM Corp., Publication No. GH20-0205.
21. Jeffrey, A. 1985. Mathematics for Engineers and Scientists. 3rd ed. Van Nostrand Reinhold, London. 707.
22. Rich, P. R. 1981. Electron transfer reactions between quinols and quinones in aqueous and aprotic media. *Biochim. Biophys. Acta.* 637:28–33.
23. Chapman, D. J., J. De Felice, and J. Barber. 1983. Influence of winter and summer growth conditions on leaf membrane lipids of Pisum sativum. *Planta.* 157:218–223.
24. Crane, F. L. 1959. Isolation of two quinones with coenzyme Q activity from alfalfa. *Plant Physiol.* 34:546–551.
25. Newman, G. C., and C. Huang. 1975. Structural studies on phosphatidylcholine-cholesterol mixed vesicles. *Biochemistry.* 14:3363–3370.
26. Blackwell, M. F., K. Gounaris, and J. Barber. 1986. Evidence that pyrene excimer formation in membranes is not diffusion-controlled. *Biochim. Biophys. Acta.* 858:221–234.
27. Blackwell, M. F., and K. Gounaris. 1985. Plastoquinone photolysis in protic and aprotic solvents and in model membranes. *Biochem. Soc. Trans.* 14:51–52.
28. Turro, N. J. 1978. Modern Molecular Photochemistry. The Benjamin-Cummings Publishing Co., Menlo Park, CA. Chap. 9.
29. Blackwell, M. F., K. Gounaris, and J. Barber. 1987. Plastoquinol and plastoquinone diffusion in model membranes. *In* Proceedings VII International Congress on Photosynthesis. J. Biggins, editor. Martinus Nijhoff, The Netherlands. In press.
30. Ort, D. A. 1986. Energy transduction in oxygenic photosynthesis: an overview of structure and mechanism. *In* Photosynthesis III. Vol. 19. Encyclopedia of Plant Physiology. L. A. Staehelin and C. J. Arntzen, editors. Springer-Verlag GmbH & Co., Heidelberg, Berlin. 143–196.